Indian Journal of Chemical Technology
Vol. 25, January 2018, pp. 21-30

Polyethylene quality control in an industrial scale fluidized bed reactor

Omid Vahidi*[1] & Mohammad Shahrokhi[2]

[1]School of Chemical Engineering, Iran University of Science and Technology, Narmak, Tehran, Iran
[2]Chemical and Petroleum Engineering Department, Sharif University of Technology,
P.O. Box: 11155-9465, Tehran, Iran

E-mail: ovahidi@iust.ac.ir

Received 2 June 2016; accepted 23 October 2016

Polymer quality control in an industrial scale polyethylene fluidized bed reactor has been addressed. Since online measurements of polymer properties (melt index and density) are not available, they must be controlled indirectly via other available measurements. In the present paper, two algebraic equations correlating polyethylene melt index and density with the measureable concentrations of chemical components are obtained. Having the desired polyethylene properties and using these correlations, desired concentrations of chemical components are calculated and used via corresponding control loops. By using the infrequently available polyethylene property measurements, the correlation parameters are updated. In order to simulate the fluidized bed reactor behaviour, a comprehensive two phase model including bubble and emulsion phases is used. Six control loops with PI controllers are considered to regulate the reactor operating conditions. To improve the performances of the component concentration loops, ratio control strategy in a cascade framework is implemented. The effectiveness of proposed reactor control structure for several scenarios comprising the rejection of operational disturbances, set-point tracking for polyethylene production amount and grade changes and compensating the model uncertainties is demonstrated via computer simulation. The results indicate that the polyethylene properties are well controlled with the proposed inferential control strategy.

Keywords: Fluidized bed reactor, Inferential control, Polyethylene quality control, Ratio control, Two-phase model

Nowadays, polyethylene is considered to be the world largest produced polymer in petrochemical plants[1]. Because of advantages of gas-phase processes such as moderate reaction operating conditions, absence of solvents and well mixing of the components, polyolefin production with several quality specifications through heterogeneous Ziegler-Natta catalysts in fluidized bed reactor (FBR) has been recognized as one of the most efficient processes for olefin polymerization in petrochemical plants[2].

Due to the high nonlinearity of polymerization reactions, the strong interaction between the reactor variables and possible instability of reactor operating conditions, control of polymerization reactions in FBR has been known a challenging problem. However, there are relatively few works regarding control of gas-phase polymerization of ethylene in fluidized-bed reactors. Most of these works are limited to the reactor temperature stability and control[3-8]. In a few works, more than one control variable has been considered. McAuley and McGregor[9] have studied control of the polymer quality variables (i.e. melt flow index and density) by manipulating the feed flows and have compared the performances of a linear internal model controller (IMC) and a nonlinear feedback controller. Shamiri *et al.* have controlled the polymer production rate and the reactor temperature using model predictive controller[10] and adaptive predictive model-based control[11]. Ali *et al.*[12] have proposed a control scheme in which the monomer conversion and melt index of produced polymer are controlled via manipulating the reactor cooling water flow and the inlet hydrogen concentration. In another work, Ali *et al.*[13] have investigated control of the reactor temperature and pressure in addition to the gas partial pressures. They have compared performances of two different multivariable control approaches. Chatzidoukas *et al.*[14], Bonvin *et al.*[15] and Fei *et al.*[16] have studied the optimal grade transition problem for a polyethylene FBR.

In the present study, based on a comprehensive model, polymer quality control in a gas-phase ethylene 1-butene copolymerization FBR using Ziegler-Natta catalyst has been considered. The paper is organized as follows. First, the process description and the mathematical modelling of polyethylene production in FBR are described. Next, the algebraic correlations for prediction of polymer properties from process variables are given and a recursive parameter

estimation technique is used to update the correlation parameters when infrequent laboratory measurements become available. Then, control of reactor operating conditions is discussed and product quality control is also investigated. To improve the performances of concentration control loops, some modifications are proposed. Finally results and conclusion are drawn.

Experimental Section

Modeling of the polyethylene production in a FBR

The schematic flow diagram of ethylene copolymerization in a FBR is shown in Fig. 1. A gas stream containing four components (ethylene, 1-butene, hydrogen and nitrogen) is fed continuously to the bottom of the reactor through a distributor. Catalyst particles are fed to the reactor at a point above the distributor. Through the reactor bed, via contact of catalyst particles and gas components, polymer is produced. Polymer particles are withdrawn at a point above the catalyst inlet approximately below the middle of the reactor. Because of low conversion, outlet unreacted gas from top of the reactor is recycled to the reactor continuously. Since the polymerization reaction is exothermic, an external heat exchanger is employed for removal of the heat generated by polymerization reaction from the recycled gas. In industrial plants it is common to recycle the exchanger outlet water and control the reactor temperature by manipulating the mass flow of cooling water supply (Fig. 1).

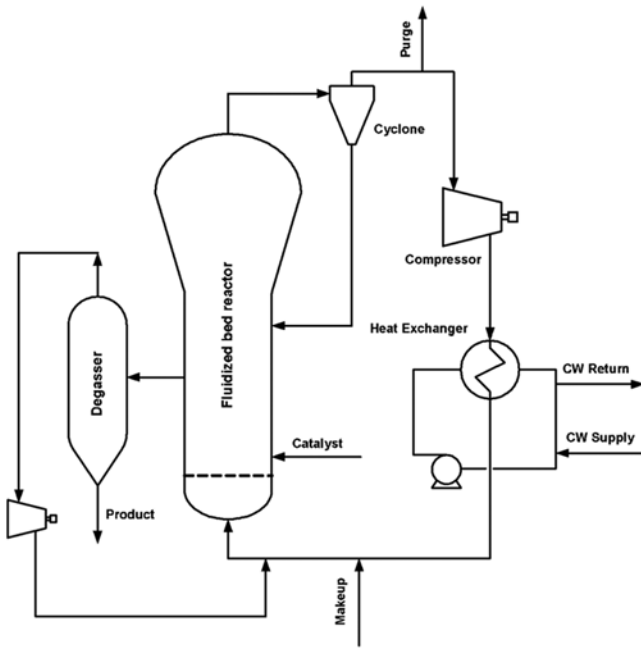

Fig. 1 — Schematic diagram of a fluidized bed polyethylene reactor and its upstream and downstream units.

Reaction kinetics

Olefin polymerization modeling over the Ziegler-Natta catalyst has been the subject of many studies in two recent decades[14,17-21]. In the present study, a comprehensive model is considered to describe the ethylene copolymerization kinetics over the Ziegler-Natta catalyst. This model is based on the assumption of catalyst with multiple active sites. Table 1 shows the mechanism of copolymerization kinetics[21].

The reaction rates of each component participating in copolymerization reactions are given in Table 2[21]. The symbol $N_{r,i}^{j}$ indicates the concentration of live copolymer chains of length r in j^{th} site ending with i^{th} monomer and $N_{0,H}^{j}$ denotes the concentration of live copolymer chains of zero length in j^{th} site generated due to transfer reaction with hydrogen.

In the kinetic reaction rates, the pseudo-kinetic constants are used[21,22]. The v^{th} moment of live and dead polymer chains in j^{th} site are Y_{v}^{j} and X_{v}^{j} and given by:

Table 1 — Ethylene and 1-butene copolymerization kinetics over the Ziegler-Natta catalyst[21]

Formation by cocatalyst	$S_p^j + C \xrightarrow{kf^j} N_0^j$
Initiation	$N_0^j + M_i \xrightarrow{ki_i^j} N_{1,i}^j$
Propagation	$N_{r,i}^j + M_k \xrightarrow{kp_{ik}^j} N_{r+1,k}^j$
Transfer to monomer	$N_{r,i}^j + M_k \xrightarrow{ktm_{ik}^j} N_{1,k}^j + D_r^j$
Transfer with hydrogen	$N_{r,i}^j + H_2 \xrightarrow{kth_i^j} N_{0,H}^j + D_r^j$
Reinitiation with monomer	$N_{0,H}^j + M_i \xrightarrow{kih_i^j} N_{1,i}^j$
Transfer with cocatalyst	$N_{r,i}^j + C \xrightarrow{ktc_i^j} N_{1,1}^j + D_r^j$
Spontaneous transfer	$N_{r,i}^j \xrightarrow{kts_i^j} N_0^j + D_r^j$
Spontaneous deactivation	$N_{r,i}^j \xrightarrow{kds^j} N_d^j + D_r^j$
Spontaneous reactivation	$N_d^j \xrightarrow{kas^j} N_0^j$
Reaction with impurity	$N_{r,i}^j + I \xrightarrow{kdI^j} N_{0,dIH}^j + D_r^j$
Reaction with impurity	$N_0^j + I \xrightarrow{kdI^j} N_{dI}^j$
Reaction with impurity	$N_{0,H}^j + I \xrightarrow{kdI^j} N_{0,dH}^j$

Table 2 — Reaction rates of various molecular species[21]

$$R^j_{S_p} = -kf^j[C]S^j_p$$

$$R^j_{N_0} = kf^j[C]S^j_p + ka^j N^j_d - N_0\{ki^j_T[M_T] + kas^j + KdI^j[I]\}$$

$$R^j_{N_{0,H}} = Y^j_0\{kth^j_T[M_3] + kts^j_T\} - N^j_{0,H}\{kih^j_T[M_T] + kds^j + KdI^j[I]\}$$

$$R^j_{N_{1,1}} = \{ki^j_1 N^j_0 + kih^j_1 N^j_{0,H} + ktm^j_{T1}Y^j_0\}[M_1] + ktc^j_T Y^j_0[C]$$

$$-N^j_{1,1}\{kp^j_{1T}[M_T] + ktm^j_{1T}[M_T] + kth^j_1[M_3] + ktc^j_1[C] + kts^j_1 + kds^j + KdI^j[I]\}$$

$$R^j_{N_{1,2}} = \{ki^j_i N^j_0 + kih^j_i N^j_{0,H} + ktm^j_{Ti}Y^j_0\}[M_2] - N^j_{1,2}\{kp^j_{2T}[M_T]$$

$$+ktm^j_{2T}[M_T] + kth^j_2[M_3] + ktc^j_2[C] + kts^j_2 + kds^j + KdI^j[I]\}$$

$$R^j_{Y_0} = [M_T]\{ki^j_T N^j_0 + kih^j_T N^j_{0,H}\} - Y^j_0\{kth^j_T[M_3] + kts^j_T + kds^j + KdI^j[I]\}$$

$$R^j_{Y_1} = [M_T]\{ki^j_T N^j_0 + kih^j_T N^j_{0,3}\} + \{Y^j_0 - Y^j_1\}\{ktm^j_{TT}[M_T] + ktc^j_T[C]\}$$

$$+[M_T]kp^j_{TT}Y^j_0 - Y^j_1\{kth^j_T[M_3] + kts^j_T + kds^j + KdI^j[I]\}$$

$$R^j_{Y_2} = [M_T]\{ki^j_T N^j_0 + kih^j_T N^j_{0,H}\} + \{Y^j_0 - Y^j_2\}\{ktm^j_{TT}[M_T] + ktc^j_T[C]\}$$

$$+[M_T]kp^j_{TT}\{2Y^j_1 - Y^j_0\} - Y^j_2\{kth^j_T[M_3] + kts^j_T + kds^j + KdI^j[I]\}$$

$$R^j_{X_\nu} = \{Y^j_\nu - N^j_{1,T}\}\{ktm^j_{TT}[M_T] + ktc^j_T[C]kth^j_T[M_3] + kts^j_T + kds^j + KdI^j[I]\} \quad \nu = 0,1,2$$

$$R^j_{N_d} = \{N^j_0 + N^j_{0,H}\}kd^j + kd^j_T Y^j_0 - ka^j N^j_d$$

$$R_{M_i} = \sum_{j=1}^{s}[M_i]Y^j_0 Kp^j_{Ti} \qquad i = 1,2$$

$$R_{M_3} = \sum_{j=1}^{s}[M_3]Y^j_0 Kth^j_T$$

$$R_I = \sum_{j=1}^{s}[I]KdI^j([Y^j_0 + N^j_0 + N^j_{0,H}])$$

$$Y^j_\nu = \sum_{i=1}^{m}\sum_{r=1}^{\infty} r^\nu[N^j_{r,i}], \quad X^j_\nu = \sum_{r=1}^{\infty} r^\nu[D^j_r] \qquad \text{... (1)}$$

The kinetic rate constants and corresponding activation energy are given in Table 3 (Ref. 14,19).

Reactor hydrodynamic modeling

For polyethylene production in FBRs, models such as single-phase continuous stirred tank reactor (CSTR), two-phase model including bubble[23] and emulsion phases[4,19,24-27] and heterogeneous three-phase plug flow reactor[2,28] have been used. Hatzantonis *et al.*[19] in a research work developed the two phase model by considering the bubble growth effect on hydrodynamic behaviour of the reactor and showed that the developed model has a better agreement with industrial data compared to single and two phase models with constant bubble size.

In the present study, a two phase model including bubble and emulsion phases which considers the bubble growth effect is used. The model is described in Vahidi *et al.*[29] and the readers are referred to this reference for more details.

Estimating polymer properties from reactor process variables

In petrochemical plants, a common problem associated with polymerization units is the lack of online measurements of polymer properties (i.e. density and melt index)[30]. The online available measurements of reactor operating conditions are usually pressure, temperature and gas composition while different grades of polymers are recognized by their density and melt index whose online measurements are not normally available. McAuley and MacGregor[31] have proposed a model to predict polyethylene properties from online measurement of reactor variables. They have employed recursive parameter estimation technique and the extended Kalman filter to update the model parameters by offline measurement of polymer quality variables. The estimated values of polymer density and melt index have been used for control purposes. Recently

Table 3 — Kinetic rate constants for copolymerization reactions

	Site type 1	Site type 2		Site type 1	Site type 2
Formation			Chain transfer		
kf^j	1×10^2	1×10^2	ktm_{11}^j	2.1	2.1
E_f^j	9	9	ktm_{12}^j	6	1.1×10^2
Initiation			ktm_{21}^j	2.1	1
ki_1^j	1×10^3	1×10^3	ktm_{22}^j	6	1.1×10^2
ki_2^j	1.4×10^2	1.4×10^2	kth_1^j	88	3.7×10^2
$E_{i,k}^j$	9	9	kth_2^j	88	3.7×10^2
Propagation			ktc_1^j	24	1.2×10^2
kp_{11}^j	8.5×10^4	8.5×10^4	ktc_2^j	48	2.4×10^2
kp_{12}^j	2×10^3	1.5×10^4	kts_1^j	1×10^{-4}	1×10^{-4}
kp_{21}^j	6.4×10^4	6.4×10^4	kts_2^j	1×10^{-4}	1×10^{-4}
kp_{22}^j	1.5×10^3	6.2×10^3	E_t^j	8	8
$E_{p,ik}^j$	9	9	Deactivation		
Reinitiation			kd^j	0.1	0.1
kih_1^j	1×10^3	1×10^3	kdI^j	2×10^6	2×10^6
kih_2^j	1×10^2	1×10^2	E_d^j	8	8
$E_{ih,k}^j$	9	9	Reactivation		
			ka^j	3×10^{-4}	3×10^{-4}
			E_d^j	9	9

Rallo *et al.*[32] and Sharmin *et al.*[33] have also proposed some soft sensors for predicting the polymer properties from process variables.

In the present study, correlations which relate polymer properties to compositions in the reactor are obtained. By using these correlations, desired values of reactor compositions can be calculated from the required polymer properties and used for control purposes.

McAluely and McGregor investigations, static simulations performed with different models (well mixed model and the model introduced in previous section) and the industrial data indicate that among different process variables, the ratio of component concentrations in the reactor and reactor temperature have the most significant effects on the polymer quality variables. Since FBRs are operated in a narrow temperature range, the temperature effect on polymer quality variables is ignored.

To obtain correlations between polymer quality variables and ratio of concentrations, a set of off-line data is needed. These data have been obtained from static simulation using the comprehensive model introduced in the previous section. In industry, for controlling the polyethylene properties (i.e. density and melt index), hydrogen and 1-butene to ethylene concentration ratios are controlled[31]. If correlations between these ratios and polymer properties are available, they can be used for control purposes. Although polymer properties are functions of aforementioned concentration ratios, in this work it has been tried to relate concentration ratios to polymer properties for ease of control implementation. Having the desired polymer properties and such correlations, the required concentration ratios of hydrogen and 1-butene to ethylene are calculated and used as set-points for corresponding control loops. To obtain such relations, concentration ratio of hydrogen to ethylene versus polymer melt index (MI) at different polymer densities and also variations of concentration ratio of 1-butene to ethylene versus polymer density at different polymer MIs are shown in Fig. 2.

The data shown in Fig. 2, indicates that there exist one to one maps between concentration ratios and polymer properties. The following correlations have been proposed:

$$\frac{[M_2]}{[M_1]} = a_1\rho^2 + a_2\rho + a_3 \quad \ldots (2)$$

$$\frac{[H_2]}{[M_1]} = b_{11}MI^2 + b_{22}\rho^2 + b_{12}\rho MI + b_1 MI + b_2\rho + b_3 \quad \ldots (3)$$

where H_2, M_1 and M_2 are concentrations of hydrogen, ethylene and 1-butene, respectively. To update the parameters of the above equations by using infrequent laboratory measurements, the recursive least squares (RLS) algorithm is employed:

$$\theta(k) = \theta(k-1) + \frac{P(k-1)\varphi(k)e(k)}{1+\varphi^T(k)P(k-1)\varphi(k)} \quad \ldots (4)$$

$$P(k) = P(k-1) + \frac{P(k-1)\varphi(k)\varphi^T(k)P(k-1)}{1+\varphi^T(k)P(k-1)\varphi(k)} \quad \ldots (5)$$

where e is the vector of estimation error and P is the covariance matrix. θ is the vector of parameters and

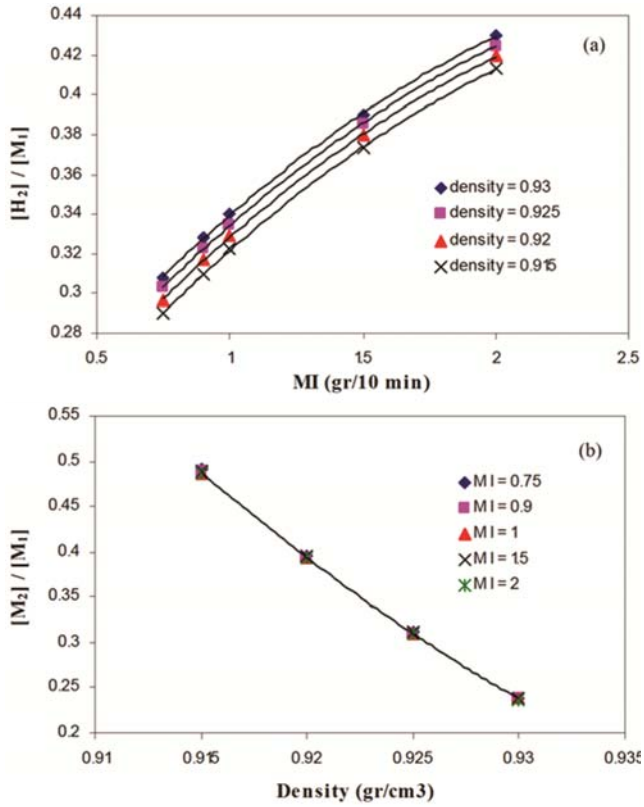

Fig. 2 — Concentration ratios versus polyethylene properties, (a) concentration ratio of hydrogen to ethylene versus polyethylene melt index at different polyethylene densities, (b) concentration ratio of 1-butene to ethylene versus polyethylene density at different polyethylene melt indices.

φ is the vector of laboratory measurements as given below:

$$\theta_1^T = [a_1\ a_2\ a_3], \theta_2^T = [b_{11}\ b_{22}\ b_{12}\ b_1\ b_2\ b_3] \quad \ldots (6)$$

$$\phi_1^T(k) = [\rho^2\ \rho 1], \phi_2^T(k) = [MI^2\ \rho^2\ MI\rho\ MI\ \rho 1] \quad \ldots (7)$$

FBR control structure

For reactor stability and operability, the reactor temperature, pressure and the bed height must be controlled at specified points. To control the polymer quality variables at desired values, the concentration ratio of 1-butene and hydrogen to ethylene must be maintained at specified values determined by equations (2) and (3) and desired polymer density and MI. Finally, to maintain the reactor production rate at a desired value, the ethylene concentration should be controlled.

To control the above process variables, nine manipulated variables are available. These variables are the makeup streams flow rates (ethylene, 1-butene, hydrogen and nitrogen), flow rate of bleed stream, cooling water makeup flow rate, polymer withdrawal mass flow rate, catalyst mass flow rate and the gas recycle stream flow rate. In polymer industries, it is common to maintain catalyst, bleed stream and gas recycle stream flow rates at fixed specified values. Therefore, six manipulated variables are practically available to control the reactor process variables.

Table 4 — Loop pairings between manipulated and controlled variables

Controlled variable	Manipulated variable
Ethylene concentration	Ethylene makeup feed rate
1-butene concentration	1-butene makeup feed rate
Hydrogen concentration	Hydrogen makeup feed rate
Temperature	Cooling water makeup feed rate
Pressure	Nitrogen makeup feed rate
Bed height	Polymer withdrawal rate

Optimal selection of closed-loop controllers has been investigated by Chatzidoukas *et al.*[14] They selected control pairings based on relative gain array (RGA) algorithm. In the present study, six single input single output (SISO) control loops are considered. The control pairings are shown in Table 4.

For each control loop, a conventional PI controller with anti-windup[34] is considered. Tuning of the controller parameters are accomplished based on maximum 10% overshoot for each loop while the other loops are open. To handle the loop interactions, the detuning procedure proposed by Luyben[35] has been used. To improve the performances of concentration ratio loops, flow ratio control strategy in a cascade framework, described below, has been used.

A common disturbance in industrial plants is the upset in the pressure of feed streams. This will affect the reactor compositions and consequently the polymer properties. For damping the effect of this load, the cascade control strategy can be used. In this control strategy the master controller is the concentration ratio control and the slave controller is the flow control. The volumetric flow rate determined by control valve is given by the Ramirez: [36]

$$F = Kv\sqrt{P_{up}(P_{up} - P_{down})} \quad \ldots (8)$$

where F is the volumetric flow rate of gas passing through the valve, P_{up} and P_{down} denote the upstream and downstream pressures and Kv is the valve coefficient which is a function of valve opening percentage.

The effect of upset in the ethylene line can be damped faster if in the inner loops of hydrogen and

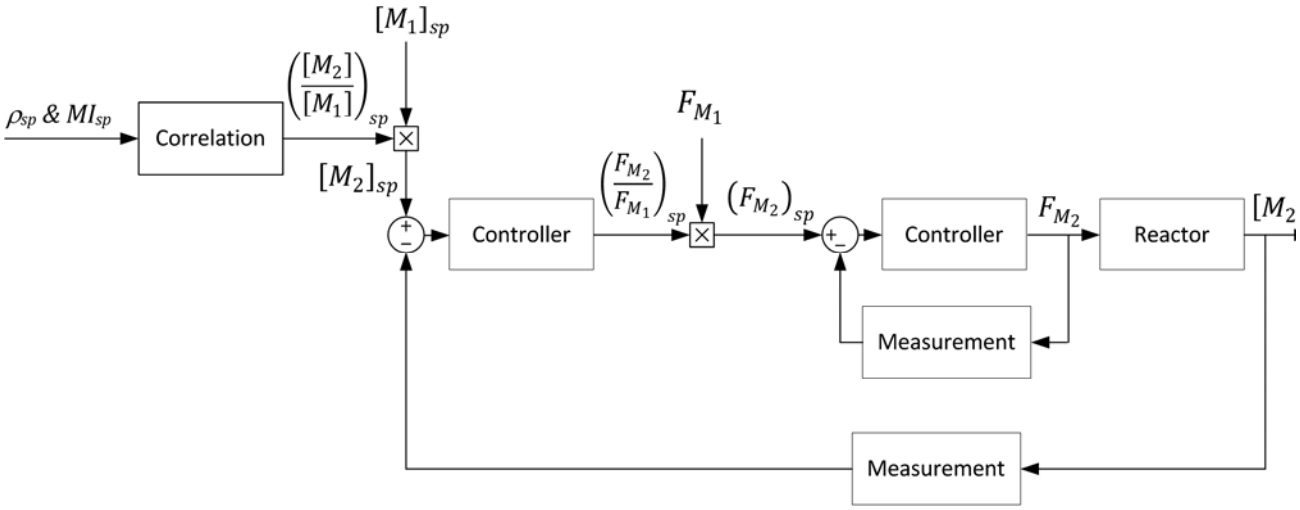

Fig. 3 — Combination of cascade and ratio control structures for ratio concentration loops.

1-butene, flow ratio control strategy is used. Figure 3 shows the block diagram for implementation of this strategy for 1-butene. Hydrogen concentration loop has a similar structure. Having the desired values of polymer MI and density and using correlations (2) and (3), the desired composition ratios for hydrogen and 1-butene are obtained. Multiplying these ratios by the measured ethylene concentration, the desired hydrogen and 1-butene concentrations are calculated and used in composition loops as the desired set-points. The master controllers provide the desired flow rate ratios. Multiplying these flow ratios by the ethylene desired flow, the flow rate set-points of the slave loops are obtained.

Results and Discussion

To check the accuracy of the model, a static simulation is performed and its result is compared with that of an industrial petrochemical plant. The required physical parameters and operational conditions are given in Table 5. The results of static simulation and the corresponding industrial data are given in Table 6. As can be seen, there is a good agreement between simulation and industrial data.

In what follows, dynamic simulation by using the comprehensive model is considered. Through dynamic simulation, the performances of parameter estimators are evaluated for load rejection, set-point tracking and system regulation under model uncertainty. In the case of load rejection, the control performances for various control strategies are investigated.

Dynamic simulation is accomplished by solving the model equations. The model introduced in the first section contains 5 partial differential equations, 37 ordinary differential equations and many algebraic relations employed to calculate the various model parameters. To solve this set of equations, backward difference method is used to discretize the partial differential equations with respect to reactor length. The resulting ordinary differential equations are solved using the Runge Kutta method. In dynamic

Table 5 — Parameters used for static simulation

Physical parameters	Operating Conditions
Cp_1 = 1.86 J/g.K	$makeup_1$ = 3623.6 g/s
Cp_2 = 2.76 J/g.K	$makeup_2$ = 524.6 g/s
Cp_{33} = 14.25 J/g.K	$makeup_3$ = 4.17 g/s
Cp_4 = 1.07 J/g.K	$makeup_4$ = 144.5 g/s
Cp_p = 1.91 J/g.K	bleed = 0.002× $\dot{m}_{Rec}$
d_p = 0.05 cm	$\dot{m}_{cat}$ = 0.01 g/s
D_g = 0.004 cm^2/s	$\Delta P_{compressor}$ = 0.77 bar
ΔH_1 = 3829 J/g	$\dot{m}_w$ = 8.4×10^5 g/s
ΔH_2 = 3843 J/g	polymer withdrawal = 3722.2 g/s
ρ_{cat} = 1.91 J/g.K	
T_{ref} = 300.15 K	

Table 6 — Simulation results and the corresponding industrial data

	Industrial data	Two phase model
T	349	348.5
P	20.0	20.03
$y_{1\text{-}O}$	0.445	0.449
$y_{2\text{-}O}$	0.196	0.198
$y_{3\text{-}O}$	0.099	0.099
$\overline{M}w$	9.7×10^4	11.2×10^4
ρ_p	0.920	0.916
MI	0.9	0.98

simulation study, four minutes delay is considered for concentration measurements and it is assumed that polymer density and MI are available every 1 h.

Load rejection

As mentioned before, a common disturbance in industrial plants is the feed stream pressure fluctuations. To evaluate the performance of the proposed control structure in load rejection, the upstream pressure of ethylene feed stream has been increased by 5 bar. Figure 4 (a) and (b) shows variations of polymer MI and density resulted from the proposed control scheme compared with a conventional single loop PI controller.

Increasing the upstream pressure of the ethylene feed flow results in a higher ethylene flow rate into the reactor which in turn leads to the elevated ethylene concentrations resulting in the lowered polymer density and elevated polyethylene MI (according to Fig. 2). This trend is predicted by simulation (see Fig. 4 (a) and (b)). The results indicate that the performance of the cascade plus ratio control strategy is much better than that of single concentration loop. The improvement is mainly due to the faster load rejection accomplished by the inner loop of the cascade controllers which return the concentrations of chemical components present into the reactor to their desired values.

In the second case, the effect of impurity on the performance of the proposed controller with and without parameter estimator is investigated. In industrial plants, presence of impurities in inlet streams is unavoidable. Some of these impurities can deteriorate the reactor performance significantly. The effect of such impurities is considered in polymerization kinetics (Table 1). For the second case, it is assumed that a continuous stream of impurity enters the reactor and its concentration in the reactor remains constant at 1e-4 mol/m^3. Under this condition, variations of polyethylene properties using proposed controller with and without parameter estimator are shown in Fig. 4 (c) and (d).

As can be seen, when parameter estimator is active the polymer properties return to their desired values while there are offsets in polymer properties when the estimator is off. Since the presence of impurity results in an equal decrease in ethylene and 1-butene consumption rates, the offset corresponding to polymer density is negligible with respect to that of the melt index.

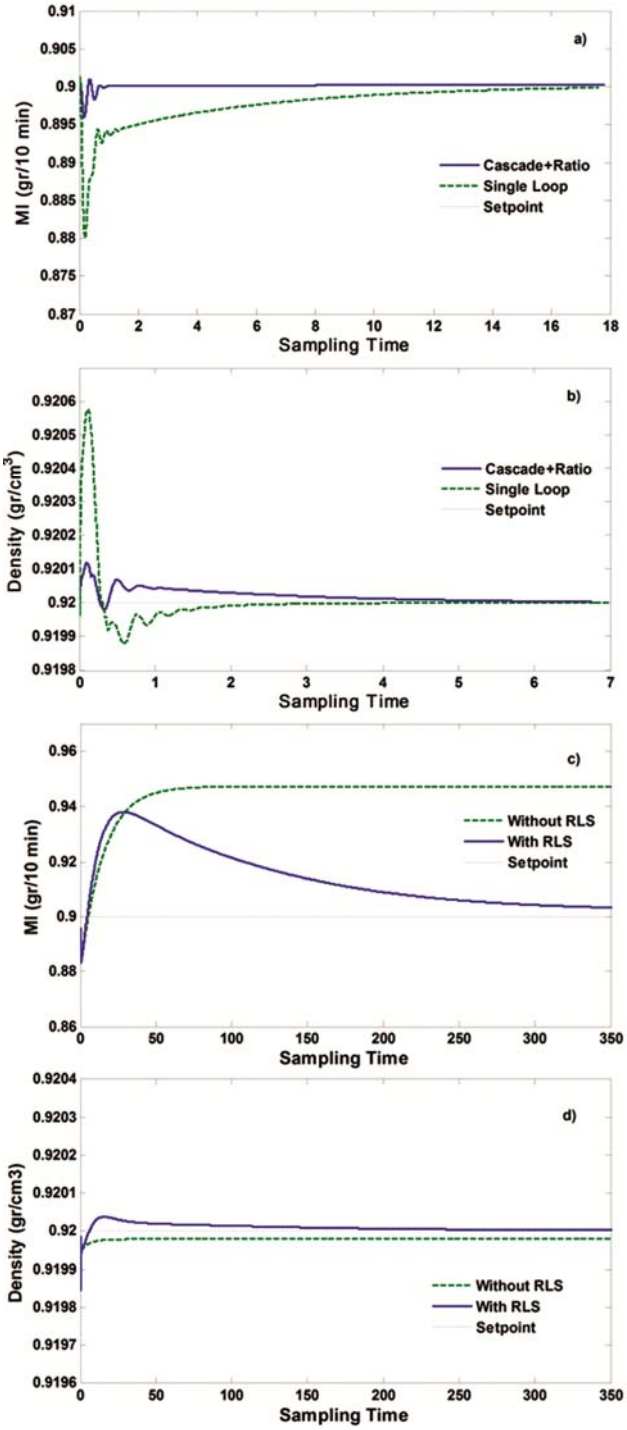

Fig. 4 — Variations of polyethylene melt index and density due to the occurrence of operational loads; (a) and (b) the operational load of 5 bar upset in ethylene upstream pressure; (c) and (d) the operational load due to the entrance of impurity into the reactor

Set-point tracking

In this part, performance of the RLS parameter estimation is evaluated for two cases. In the first case,

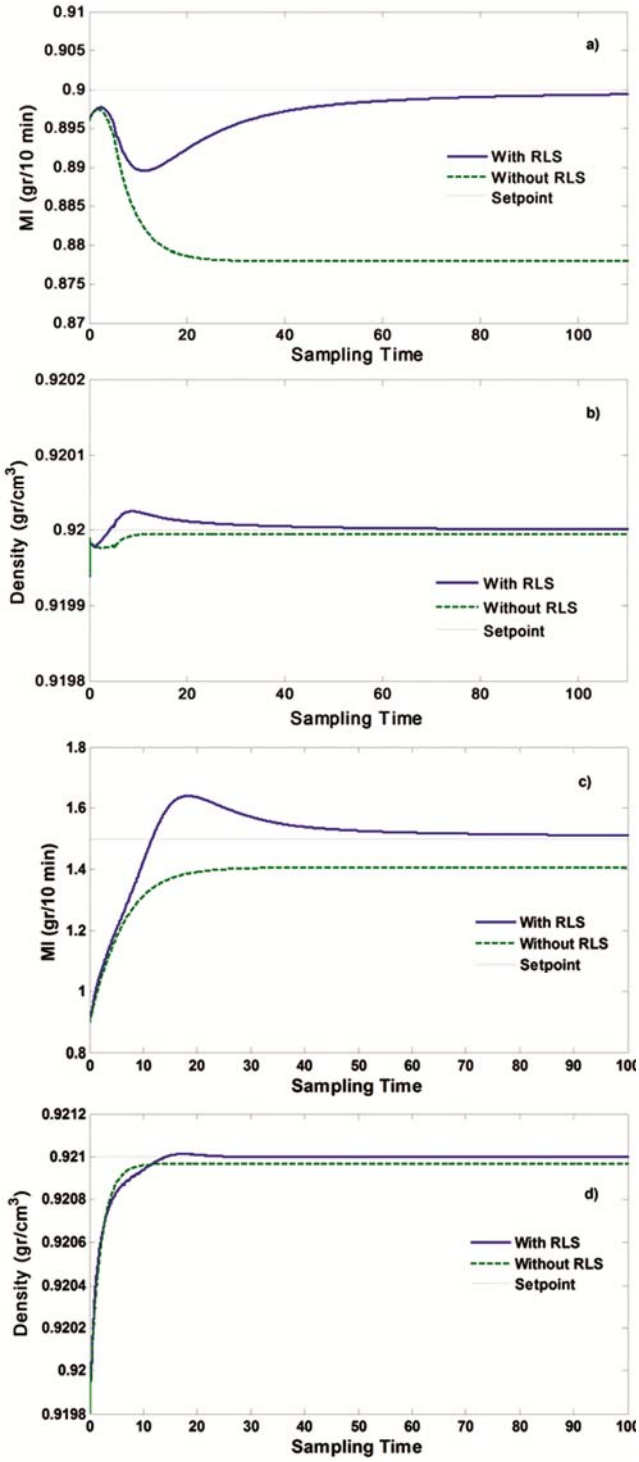

Fig. 5 — Variations of polyethylene melt index and density due to the set-point change; (a) and (b) 30% increase in the reactor productivity; (c) and (d) polyethylene grade change from grade A to grade B as indicated in Table 7.

the production rate of the reactor is increased by 30 percents. Variations of polyethylene quality variables are shown in Fig. 5 (a) and (b). To increase the production rate, the ethylene concentration set-point is increased by 30 percents and the set-points of 1-butene and hydrogen are adjusted accordingly. Since the correlations represented by equations (2) and (3) are not exact, when the parameter estimator is off, the error in correlations causes the produced polyethylene melt index and density converge to undesired variables.

Table 7 — Polyethylene Grade change specification

	Grade A	Grade B
MI	0.9	1.5
ρ	0.92	0.921
T	349	354

In the second case, polyethylene grade change is considered. In this case, the set-points of polymer quality variables and the reactor temperature are changed from grade A to grade B. The information for both grades is indicated in Table 7. To perform the grade change, the new desired values of polyethylene melt index and density are put in equations (2) and (3) and new desired ratios for concentration ratios of chemical components are calculated and used for the concentration control loops.

Figure 5 (c) and (d) shows variations of the polymer quality variables due to grade change. As can be seen, for both cases there are offsets in polymer properties when the parameter estimator is off. The density offset is less for both cases, which means that polymer density is less affected by variations of concentration ratios and operating conditions.

Model uncertainty

Finally, performance of the proposed controller coupled with parameter estimator is investigated under model uncertainty. The kinetic constants (kp_{11}^{j}, kp_{12}^{j}) are increased by 5 percent and the results are shown in Fig. 6.

As can be seen, increasing these kinetic constants led to an increase in polymer density and decrease in polymer MI. Since increasing these kinetics constants result in higher ethylene consumption rate, instantaneous mole percent of 1-butene in polymer decreases and consequently, the polymer density increases. On the other hand, the consumption rate of hydrogen remains constant, while the ethylene consumption rate increases

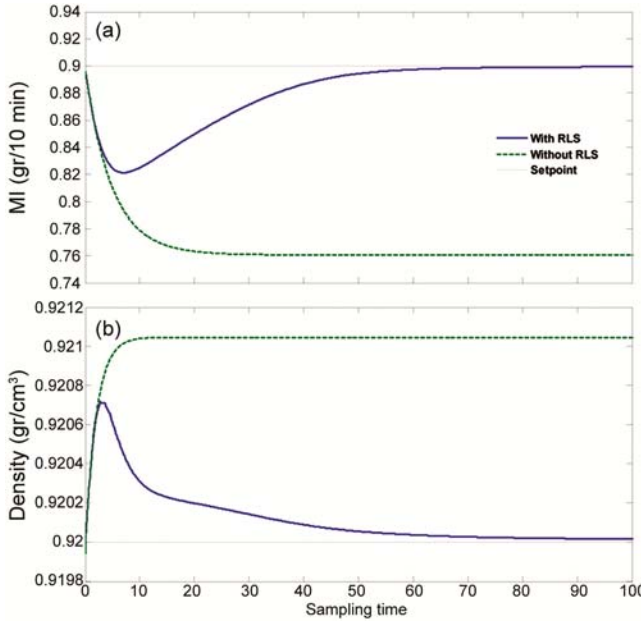

Fig. 6 — Variations of polyethylene melt index and density considering 5% error in ethylene propagation reaction rates.

which leads to a decrease in polymer MI. As can be seen from Fig. 6, model uncertainty results in significant offset in final values of density and MI when the parameter estimator is off.

Conclusion

In this study a two phase model including bubble phase with plug flow pattern and emulsion phase with CSTR flow behaviour has been used for modeling the hydrodynamic of a polyethylene fluidized bed reactor. The double active sites Ziegler-Natta catalyst model has been used to describe the polymerization reaction. Using the offline data obtained from static simulation of a comprehensive model, correlations between polymer properties and concentration ratios in the reactor have been derived which can be used for control purposes. A recursive least squares estimator has been employed to update the correlations parameters. To maintain the reactor at desired condition, six control loops have been considered. The conventional PI controllers with anti-windup have been used to control the reactor process variables. To improve the performance of control system for load rejection, cascade plus ratio control strategy has been implemented and compared with the conventional single loop. It has been shown that the performance of the proposed control strategy is superior. The performances of the RLS parameter estimator have been evaluated for load rejection, set-point tracking and system regulation subjected to model uncertainty. It has been shown that the polymer quality variables have no offset when the parameter estimator is active.

Nomenclature

A	reactor cross-sectional area, cm^2
A_{ex}	exchanger heat transfer area, cm^2
a_c	mole of active site per gram of catalyst, mol/g
Cp	specific heat, J/g.K
$[C]$	cocatalyst concentration, mol/cm^3
D	diameter, cm
D	dead polymer chain concentration, mol/cm^3
D_g	gas self-diffusion coefficient, cm^2/s
E	activation energy, kcal/mol
H	bed height, cm
Hm	overall heat transfer coefficient, $J/K.s.cm^3$
ΔH	heat of reaction, J/g
$[I]$	impurity concentration, mol/cm^3
ka	kinetic rate constant of reactivation reaction, s^{-1}
kd	kinetic rate constant of deactivation reaction, s^{-1}
kf	kinetic rate constant of formation reaction, $cm^3/mol.s$
ki	kinetic rate constant of initiation reaction, $cm^3/mol.s$
kp	kinetic rate constant of propagation reaction, $cm^3/mol.s$
kt	kinetic rate constant of chain transfer reaction, $cm^3/mol.s$
Km	overall mass transfer coefficient, s^{-1}
Kv	valve coefficient
$[M]$	gas component concentration, mol/cm^3
$[M_T]$	total monomer concentration, mol/cm^3
$\dot{m}$	mass flow rate, g/s
$\bar{m}$	average molecular weight of repeating unit in the polymer chain
MI	melt flow index, g/10min
Mw	molecular weight, g/mol
$\bar{M}w$	weight-average molecular weight
n	total number of components
N	live copolymer chains concentration, mol/cm^3
N_0	active site concentration, mol/cm^3
N_d	deactivated live copolymer chains concentration, mol/cm^3
P	pressure, bar
Q	volumetric flow rate of polymer and gas mixture withdrawn from the reactor, cm^3/s
r	polymer chain length
R	reaction rate, $mol/s.cm^3$
S	total number of active sites
S_p	potential active site concentration, mol/cm^3
T	temperature, K
U	velocity, cm/s
U_{ex}	exchanger overall heat transfer coefficient, $J/K.s.cm^3$
V	volume, cm^3
y	mole fraction
X	total concentration of dead polymer chain, mol/cm^3
Y	total concentration of live polymer chain, mol/cm^3

Greek letters

ε	bed void fraction
ρ	Density, g/cm^3
δ	volumetric ratio of bubble phase to the bed volume
ϕ	instantaneous polymer composition

Φ cumulative polymer composition
μ viscosity, gr/cm.s

Superscripts and subscripts

1 ethylene
2 1-butene
3 hydrogen
4 nitrogen
av average
b bubble phase
bed bed
cat catalyst
e emulsion phase
ex heat exchanger
g gas
in inlet
mf minimum fluidization condition
O outlet
P polymer
Rec recycle
Ref reference
W Water

References

1 Markit I, *World Analysis - Polyethylene*. Available from: https://www.ihs.com/products/world-petro-chemical-analysis-polyethylene.html.
2 Fernandes F A N & Lona L M F, Chemical Engineering Science:*16th International Conference on Chemical Reactor Engineering*, 56 (2001) 963.
3 Ali E M, Abasaeed A E & Al-Zahrani S, *Ind Eng Chem Res*, 37 (1998) 3414.
4 Choi K-Y & Harmon Ray W, *Chem Eng Sci*, 40 (1985) 2261.
5 Dadebo S A, Bell M L, McLellan P J & McAuley K B, *J Process Control*, 7 (1997) 83.
6 Ghasem N M, *Chem Eng Res Des*, 84 (2006) 97.
7 Ibrehem A S, Hussain M A & Ghasem N M, *Chin J Chem Eng*, 16 (2008) 84.
8 Shamiri A, Wong S W, Zanil M F, Hussain M A & Mostoufi N, *Chem Eng J*, 264 (2015) 706.
9 McAuley K B & Macgregor J F, *AICHE J*, 39 (1993) 855.
10 Shamiri A, Hussain M A, Mjalli F S, Mostoufi N & Hajimolana S, *Chin J Chem Eng*, 21 (2013) 1015.
11 Ho Y K, Shamiri A, Mjalli F S & Hussain M A, *J Process Control*, 22 (2012) 947.
12 Ali M A, Betlem B, Weickert G & Roffel B, *Chem Eng Proces: Process Intensification*, 46 (2007) 554.
13 Ali E, Al-Humaizi K & Ajbar A, *Ind Eng Chem Res*, 42 (2003) 2349
14 Chatzidoukas C, Perkins J D, Pistikopoulos E N & Kiparissides C, *Chem Eng Sci*, 58 (2003) 3643.
15 Bonvin D, Bodizs L & Srinivasan B, *Chem Eng Res Des*, 83 (2005) 692.
16 Fei Z, Hu B, Ye L, Zheng P & Liang J, *CIESC J*, 4 (2010) 016.
17 De Carvalho A B, Gloor P E & Hamielec A E, *Polym*, 30 (1989) 280.
18 Galvan R & Tirrell M, *Chem Eng Sci*, 41 (1986) 2385
19 Hatzantonis H, Yiannoulakis H, Yiagopoulos A & Kiparissides C, *Chem Eng Sci*, 55 (2000) 3237.
20 Hutchinson R A, Chen C M & Ray W H, *J Appl Polym Sci*, 44 (1992) 1389.
21 McAuley K B, MacGregor J F & Hamielec A E, *AICHE J*, 36 (1990) 837.
22 Hamielec A E, MacGregor J F & Penlidis A, *Makromol Chem Macromol Symp*, 10 (1987) 521.
23 McAuley K B, Talbot J P & Harris T J, *Chem Eng Sci*, 49 (1994) 2035.
24 Adli H, Mostoufi N & Ghafelebashi S M, *J Appl Polym Sci*, 122 (2011) 393.
25 Alizadeh M, Mostoufi N, Pourmahdian S & Sotudeh-Gharebagh R, *Chem Eng J*, 97 (2004) 27.
26 Kiashemshaki A, Mostoufi N & Sotudeh-Gharebagh R, *Chem Eng Sci*, 61 (2006) 3997.
27 Movahedirad S, Molaei Dehkordi A, Deen N G, Van Sint Annaland M & Kuipers J, *AIChE J*, 58 (2012) 3306
28 Fernandes F A N & Lona L M F, *Comput Chem Eng*, 26 (2002) 841.
29 Vahidi O, Shahrokhi M & Mirzaei A, *Iran J Chem Chem Eng*, 27 (2008) 87.
30 EliÃ§abe G E & Meira G R, *Polym Eng Sci*, 28 (1988) 121.
31 McAuley K B & MacGregor J F, *AICHE J*, 37 (1991) 825.
32 Rallo R, Ferre-Gine J, Arenas A & Giralt F, *Comput Chem Eng*, 26 (2002) 1735.
33 Sharmin R, Sundararaj U, Shah S, Vande Griend L & Sun Y-J, *Chem Eng Sci*, 61 (2006) 6372.
34 Bequette B W, *Process Control: Model Des Simu*, 2002.
35 Luyben W L, *Ind Eng Chem Process Des Dev*, 25 (1986) 654.
36 Ramirez W F in *Computational Methods for Process Simulation*, 2nd edn, (Butterworth Heinemann, Oxford, UK) 1997.